IEEE Photonics Journal
An IEEE Photonics Society Publication

Open Access

Ultralow-Loss Planar Si_3N_4 Waveguide Polarizers

Volume 5, Number 1, February 2013

J. F. Bauters, Student Member, IEEE
M. J. R. Heck, Member, IEEE
D. Dai, Member, IEEE
J. S. Barton, Member, IEEE
D. J. Blumenthal, Fellow, IEEE
J. E. Bowers, Fellow, IEEE

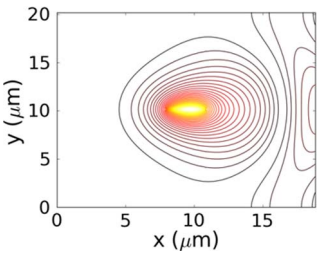

DOI: 10.1109/JPHOT.2012.2234095
1943-0655/$31.00 ©2012 IEEE

IEEE photonics SOCIETY

IEEE

Ultralow-Loss Planar Si_3N_4 Waveguide Polarizers

J. F. Bauters,[1] *Student Member, IEEE*, M. J. R. Heck,[1] *Member, IEEE*, D. Dai,[2] *Member, IEEE*, J. S. Barton,[1] *Member, IEEE*, D. J. Blumenthal,[1] *Fellow, IEEE*, and J. E. Bowers,[1] *Fellow, IEEE*

[1]Department of Electrical and Computer Engineering, University of California, Santa Barbara, CA 93106 USA
[2]Centre for Optical and Electromagnetic Research, State Key Laboratory for Modern Optical Instrumentation, Zhejiang University, Hangzhou 310058, China

DOI: 10.1109/JPHOT.2012.2234095

Manuscript received November 6, 2012; revised December 5, 2012; accepted December 9, 2012. Date of publication December 20, 2012; date of current version February 5, 2013. This work was supported by DARPA under iPhoD Contract No. HR0011-09-C-0123. Corresponding author: J. F. Bauters (e-mail: jbauters@ece.ucsb.edu).

Abstract: We demonstrate broadband (1500–1620 nm) and low-loss planar waveguide polarizers with measurement-limited on-chip extinction as high as 75 dB. Polarizers can be fabricated in higher confinement 100-nm-thick as well as lower confinement 40-nm-thick Si_3N_4 cores to suit a variety of photonic systems.

Index Terms: Waveguides, waveguide devices.

1. Introduction

Sensitivity to the optical state of polarization can limit the performance or application of photonic sensor [1] and communication [2] systems. The sensitivity typically arises from birefringence in the components of the system. To address this, one can design components with lower birefringence [3], but the lower birefringence design often requires a tradeoff with another desirable quality. In [4] and [5], for example, a square planar waveguide core having lower birefringence is shown to have higher propagation loss than a more birefringent high-aspect-ratio rectangular design. Alternatively, one can embrace polarization diversity in the system and rely on polarization splitters, polarization rotators, and polarizers for control of the polarization state. Polarization-dependent limitations are then tied to the performance of these devices.

In an optical polarizer, the loss of one polarization mode is designed to be higher than that of the other, resulting in a large polarization intensity extinction ratio after transmission through the component. In free-space systems, Glan–Thompson calcite polarizers with 50-dB extinction are available. In optical fibers, greater than 60-dB extinction due to leakage loss was demonstrated in fibers where the cladding material was partially replaced with calcite [6]. By using metal instead of calcite, an extinction of 47 dB was also demonstrated [7]. For the integration of photonic systems on a chip, planar waveguide polarizers are required. In [8], a birefringent polymer was deposited above a planar glass waveguide core, resulting in an extinction of 39 dB due to leakage loss. While in [9], proton-exchanged waveguides that guide only one polarization mode in $LiNbO_3$ allowed extinction greater than 50 dB.

In [10], we demonstrated the integration of silicon photonics with planar ultralow-loss Si_3N_4 waveguides. The combination of ultralow-loss with the active devices available in silicon enables

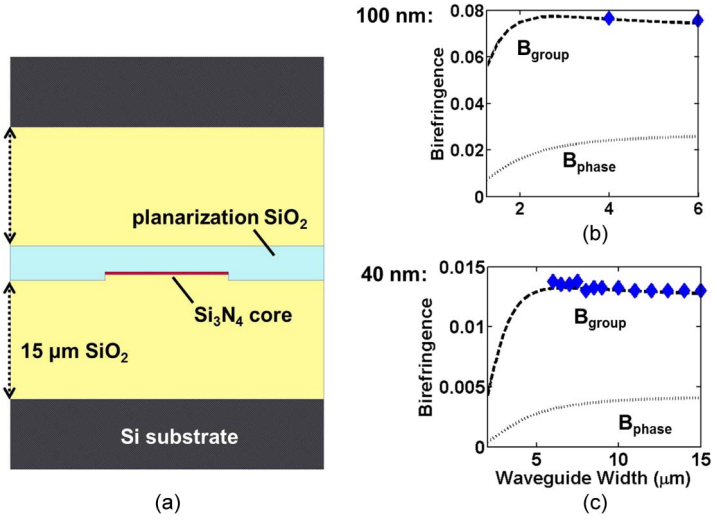

Fig. 1. (a) A schematic cross section of the planar waveguides and measured and simulated group and phase birefringence for (b) 100- and (c) 40-nm-thick cores versus waveguide width.

some integrated systems, e.g., optical gyroscopes. However, the silicon and Si_3N_4 waveguides have high birefringence such that polarization handling components are necessary. In [11], we reported polarization splitter and rotator designs in silicon waveguides. In [12], a compact silicon rib waveguide polarizer was demonstrated with an extinction as high as 25 dB. However, some applications require a polarizer with greater than 50 dB of extinction in order to achieve suitable operation [13]. In this paper, we demonstrate higher extinction (75 dB) and broadband polarizers fabricated with ultralow-loss silica waveguides. We begin with a discussion of the polarizer design and operating principle, which primarily uses a disparity in bend loss for the TE and TM modes. We then report the experimental characterization of polarizer extinction and loss using several waveguide geometries. Finally, we compare the various high-extinction results and discuss some design tradeoffs.

2. Waveguide Design and Polarizer Operating Principle

2.1. Waveguide Birefringence

Fig. 1(a) shows a schematic cross section of the planar waveguides used in this work. We study waveguides that have Si_3N_4 core thicknesses in the range of 35–100 nm. These Si_3N_4 cores are surrounded by SiO_2 cladding. The core is typically several micrometers wide in order to reduce sidewall scattering loss [4], [5]. The 15-μm-thick SiO_2 cladding layers are grown via wet thermal oxidation of Si substrates. The thinner cladding layer above the core is deposited and polished to allow for the transfer of a thick upper cladding via wafer bonding [14].

In Fig. 1(b) and (c), measured values of the group birefringence $(n_g^{\mathrm{TE}} - n_g^{\mathrm{TM}})$ for 100- and 40-nm-thick cores, respectively, are plotted versus core width. These core thicknesses are used in the polarizers discussed in Section 3. The group indices of the TE and TM modes are obtained from optical frequency-domain reflectometry measurements of waveguide backscatter near $\lambda_0 =$ 1550 nm [14]. By changing the ratio of the launched TE and TM modes with a fiber polarization controller, the TE and TM group indices can be distinguished. The dashed lines in Fig. 1(b) and (c) are simulated values for the group and phase birefringence obtained with Photon Design's FIMMWAVE mode solver at $\lambda_0 = 1550$ nm. Higher birefringence is obtained with the 100-nm-thick cores because the TE mode has high core confinement compared with the TM mode. For 100-nm-thick cores, the simulated difference in core confinement, i.e., $\Gamma_{\mathrm{TE}}^{1550\ \mathrm{nm}} - \Gamma_{\mathrm{TM}}^{1550\ \mathrm{nm}}$, is $\sim$8.8%. With decreasing core thickness, the TE confinement decreases, and the TE and TM effective indices approach the cladding index asymptote, reducing the difference in core confinement to $\sim$2.5%. The

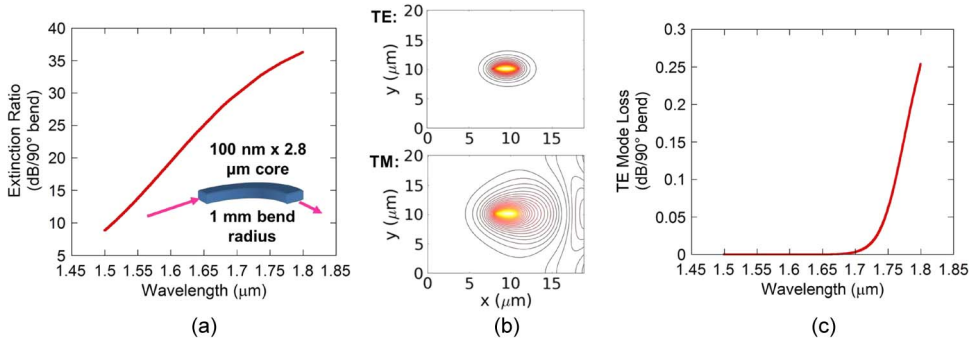

Fig. 2. (a) The simulated extinction per 90° bend obtained for 100-nm-thick cores at a 1-mm bend radius versus wavelength, (b) simulated TE and TM mode fields for $\lambda_0 = 1.65$ μm at 1-mm radius, and (c) simulated TE mode loss per 90° bend for the same radius versus wavelength.

resulting lower birefringence for 40-nm-thick cores is still greater than that typically obtained with lower index contrast elliptical core and bow-tie fibers by factors of about 25 and 3, respectively [15], [16]. The birefringence is one to two orders of magnitude lower, however, than that obtainable with higher confinement planar waveguides fabricated on 220-nm-thick silicon-on-insulator wafers.

2.2. TE/TM Loss Disparity

In [17], Varnham *et al.* showed that one linearly polarized mode in a coiled birefringent fiber becomes leaky before the other as the optical wavelength is increased. A wavelength regime then exists where the bend radiation loss is high for one polarization and low for the other, and the coil is effectively a polarizer. The difference between the wavelengths at which the TE and TM bend radiation losses begin to dominate over other loss contributions is related to the difference in TE and TM mode confinement. It is then intuitive that the operating bandwidth of the polarizer is related to the birefringence of the waveguide. In support of this, Varnham *et al.* demonstrated a 15-nm decrease in a polarizer bandwidth of 80 nm for a temperature-induced decrease in birefringence on the order of 10^{-4} [16]. Thus, the highly birefringent silica waveguides presented above would allow for an even broader bandwidth using this operating principle.

The design criteria for a TE-pass polarizer are a high TM extinction and a low TE insertion loss. Fig. 2(a) shows the TE-pass extinction ratio per 90° bend versus wavelength for a 100-nm-thick and 2.8-μm-wide planar Si_3N_4 waveguide core simulated with FIMMWAVE. The extinction increases with increasing wavelength as the TM mode confinement becomes lower and the bend radiation loss increases. The simulated mode fields shown in Fig. 2(b) illustrate the disparity in bend loss for the TE and TM modes at $\lambda_0 = 1.65$ μm. In Fig. 2(c), it is clear that the polarizer bandwidth is limited by a rapid increase in TE loss near $\lambda_0 = 1.73$ μm. For this core geometry, the simulated bandwidth of a $\geq$ 20-dB extinction polarizer with $\leq$ 0.2 dB of loss (to stay consistent with the "few percent loss" reported in [17]) is around 180 nm. Apart from the increase in bandwidth over a birefringent fiber-coil polarizer, planar processing allows greater layout flexibility for the polarizing bends. In Section 3, extinction results for several different combinations of bent and straight waveguides are reported.

3. Polarizer Characterization

3.1. Measurement Setup

In order to measure the extinction of our planar waveguide polarizers, we use a characterization setup with several polarization handling components shown schematically in Fig. 3(a). The setup is similar to that used by Suchoski *et al.* to measure polarizer extinction up to 50 dB [9]. Our setup, however, includes an automated free-space polarization controller after the tunable laser source as well as two analyzer/polarizer–detector combinations at the input and output. The polarization controller uses a polarizer, quarter-wave plate, and half-wave plate in series. The components are

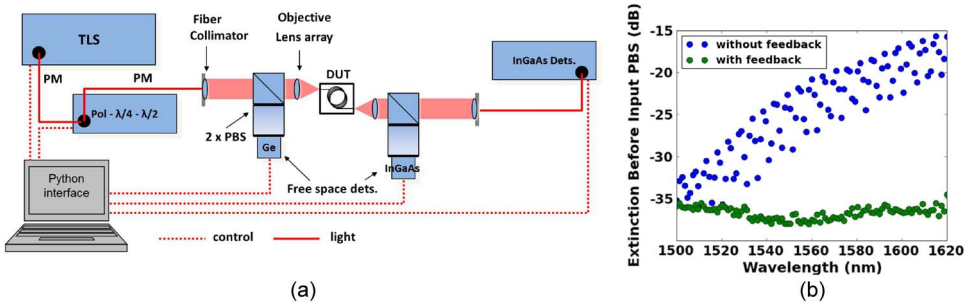

Fig. 3. (a) Schematic of the planar waveguide polarizer characterization setup with source polarization monitoring and (b) feedback results inset. For data without feedback, the polarization controller was optimized for $\lambda_0 = 1500$ nm.

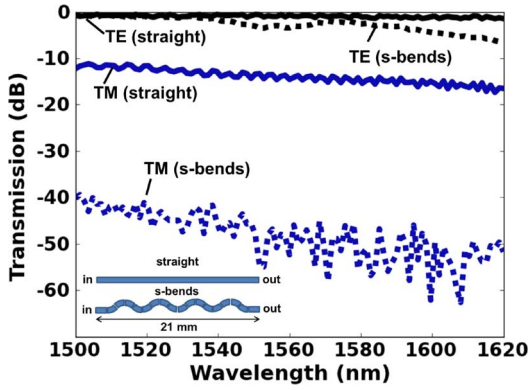

Fig. 4. TE and TM transmission through a straight waveguide and a series of s-bends with 4-μm-wide and 40-nm-thick cores.

rotated using a Python interface on a controlling computer. The Ge and InGaAs detectors in the input and output analyzers attach directly to their polarizing beam splitters via a cage system. The theoretical additive extinction of the polarization controller and two crystal polarizers is around 95 dB. However, the minimum detectable output power limits the measurable extinction of the setup to 75 dB. The input analyzer provides feedback to the controlling computer, which, in turn, adjusts the polarization controller as the wavelength of the source is swept in order to maintain a high polarization extinction at the input. Fig. 3(b) shows that the extinction of the polarization controller alone varies from 36 to 38 dB across the wavelength sweep. Fig. 3(b) also shows how the source extinction can drift by as much as 18 dB while tuning the wavelength without a feedback mechanism. The output analyzer is used to detect possible depolarization in the planar waveguide. Suchoski *et al.* reported an increase in TM transmission when the output polarizer was removed from the measurement system and attributed this increase to depolarization in their $LiNbO_3$ waveguide. Depolarization is not observed in our measurements, a finding that is consistent with the lower achievable depolarization reported for silica-based waveguide materials [18].

3.2. Polarizers With 40-nm-Thick Cores

Figs. 4 and 5 show the optical transmission through various Si_3N_4 waveguide structures fabricated with 40-nm-thick cores, using contact lithography on 100-mm Si substrates. In [14], we demonstrated that the TE propagation loss for these waveguides can be less than 0.1 dB/m for bend radii $\geq$ 6 mm. Here, we show that the TM propagation loss is much higher, enabling high-extinction polarizers. In Fig. 4, the solid lines show the TE (black) and TM (blue) transmission through straight waveguides with 4-μm-wide cores. Differing TE and TM coupling to and from the

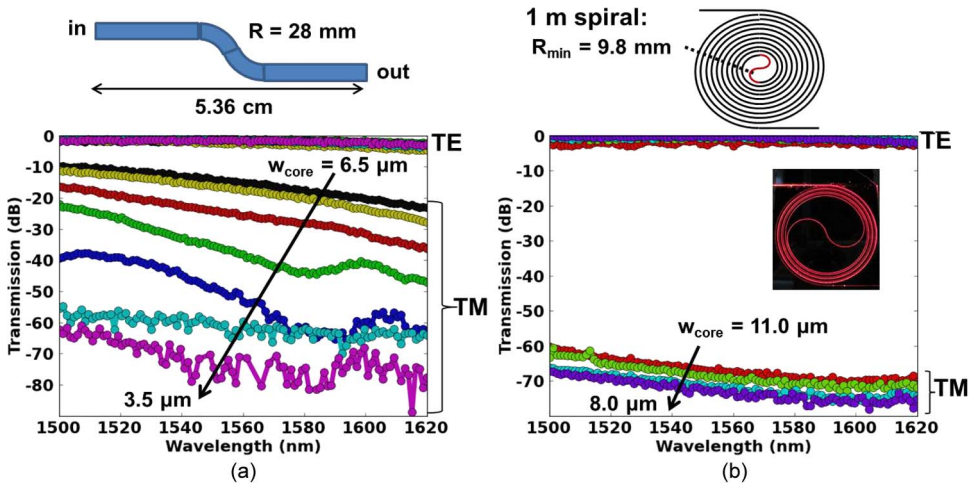

Fig. 5. (a) TE and TM transmission through a larger radius s-bend and (b) 1 m of spiraled waveguide with a 9.8-mm radius center s-bend.

free-space optics (see Fig. 3) and substrate leakage losses cause the extinction in these waveguides. Though sidewall scattering is more efficient for the TM-oriented mode field, this effect is offset by the larger TM mode size such that lower scattering loss is simulated for the TM mode. Using the cutback method, the total TM coupling loss is measured to be, at most, 3 dB greater than the total TE coupling loss. Taking this into account, a maximum on-chip polarization extinction of 12 dB is measured from 21 mm of propagation in a straight waveguide.

Fig. 4 also shows the TE and TM transmission through a series of 8 waveguide s-bends. Each bend is 9.8 mm in radius through an angle of $\sim 3.66^\circ$, and no offset between waveguides is used at bend-to-bend or straight-to-bend interfaces. The highest on-chip extinction of 42.6 dB is again measured at longer wavelengths. The TE loss for this polarizer, however, is as high as 8 dB at $\lambda_0 = 1620$ nm. This is consistent with the larger bend loss simulated and measured for narrower cores in [14]. The on-chip TE loss is reduced to below 1 dB by increasing the core width to 5 μm in the polarizer, but the average on-chip extinction is also reduced to 36.8 dB across the wavelength range. The s-bends increase the total propagation length by only 203 μm with respect to a straight waveguide, and we conclude that TM bend radiation and interface mismatch losses account for the observed increase in extinction.

Fig. 5(a) shows TE and TM transmission through a single waveguide s-bend for various core widths. Each bend is 28 mm in radius through an angle of 20.8°. The total propagation length is 54.14 mm. Because of the larger bend radius, the on-chip TE loss is less than 0.3 dB over the wavelength regime. The TM mode, however, has high substrate leakage loss over a length that is a factor of 2.58 larger than the straight waveguides in Fig. 4(a). Since the extinction is more than a factor of 2.58 larger than that measured in Fig. 4(a), we conclude that TM bend radiation and interface mismatch losses are also significant for the larger bend radius. The polarizer with a 3.5-μm-wide core has broadband on-chip extinction from 58 to 75 dB for wavelengths ranging from 1500 to 1620 nm, respectively, and less than 0.3 dB of loss for the TE mode. Fig. 5(b) shows TE and TM transmission through 1 m of spiraled waveguide. The spiral has an s-bend of 9.8-mm radius in its center. The polarization extinction for core widths narrower than 8 μm is too high to be measured with our setup. The highest measurable on-chip extinction is again 75 dB, and the TE propagation loss is lower than 0.1 dB/m near the 1580-nm wavelength regime as reported in [14].

3.3. Polarizers With 100-nm-Thick Cores

Waveguides with 100-nm-thick cores are fabricated in a CMOS foundry using 248-nm stepper lithography on 200-mm silicon substrates. TE and TM core confinement factors are higher for these thicker cores, but the same thermal oxide cladding thickness of 15 μm is used. As a result, the TE

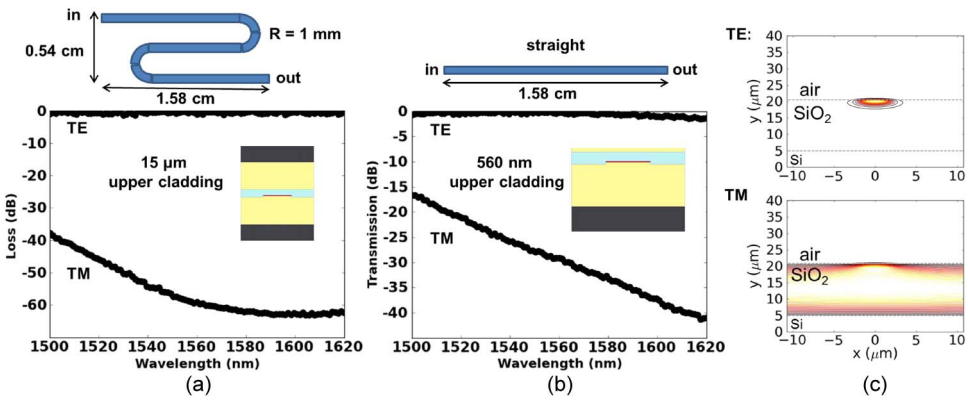

Fig. 6. (a) TE and TM transmission through an s-bend and (b) a straight waveguide with thinner upper cladding. (c) The TE and TM mode fields for the highly asymmetric waveguide with thin upper cladding.

and TM substrate leakage losses are both low. Reflectometry measurements of 6-μm-wide cores near $\lambda_0 = 1590$ nm give minimum TE and TM mode propagation losses of 1.2 and 0.6 dB/m, respectively. Though the TM mode loss is lower than that of the TE mode for larger bend radii, TM bend loss alone is high near a bend radius of 1 mm for 2.8-μm-wide cores, enabling high-extinction polarizers.

Fig. 6(a) shows the TE and TM on-chip loss measured in a single s-bend. Since the substrate leakage loss of the modes is negligible, the on-chip loss is obtained by comparing transmission through the s-bend with the average transmission through 10 straight waveguides on the same die. Broadband on-chip polarization extinction from 38 to 62 dB is measured with an average TE mode loss of 0.4 dB over the wavelength regime. One can increase the TM mode loss in the straight and bent sections by using a structure with thinner SiO_2 upper cladding, as shown schematically in the inset in Fig. 6(b), rather than bonding a 15-μm SiO_2 wafer. Such a structure is used when integrating the Si_3N_4 waveguides with Si photonics, as discussed in [10]. Fig. 6(c) shows how the TE mode remains well confined in this structure, whereas the TM mode becomes leaky. No TM power is measurable through the s-bend shown in Fig. 6(a), but the highly asymmetric structure also increases the TE bend loss at a 1-mm radius, giving a measured on-chip TE loss of 6 dB. The TE mode has low loss for larger bend radii, however, and up to 40-dB extinction due to TM leakage loss is measured in a straight waveguide, as shown in Fig. 6(b).

4. Discussion and Conclusions

We have demonstrated planar waveguide TE-pass polarizers having measurement-limited extinction ratios as high as 75 dB. The polarizers, which chiefly utilize the disparity in bend loss between TE and TM modes in a birefringent waveguide at certain bend radii, can operate with high extinction and low loss over a broad (1500–1620 nm) wavelength regime. Using 100-nm-thick cores, on-chip polarization diversity can be achieved since the loss of both polarization modes can be low at larger bend radii. This makes 100-nm-thick cores particularly attractive for applications, e.g., a coherent receiver [2], that require the chip to accept both polarizations at the input. It should be noted, however, that a TM-pass polarizer using the same operating principle cannot be realized on the same chip. Polarization splitters and/or rotators such as those discussed in [11] are then necessary. Since they have higher birefringence, a broader bandwidth polarizer should also be realizable with 100-nm-thick cores compared with thinner core designs. When the core thickness is decreased to 40 nm, however, the TM mode becomes leaky, and the TE propagation loss is less than 0.1 dB/m. This makes 40-nm-thick cores attractive for applications requiring tens of meters of propagation along with high-extinction polarizers, e.g., an interferometric optical gyroscope. As reported in [14], the coupling loss between the waveguide and an optical fiber can be lower than 1 dB per facet by tapering the waveguide core to a narrower width in order to match the fiber mode. If the

disparity between TE and TM fiber-to-chip coupling losses is a concern, a core width can be chosen such that the coupling losses are nearly equal at the cost of a slightly higher coupling loss. For example, 0.87/0.91-dB TE/TM coupling losses are simulated for 40-nm-thick and 5-μm-wide cores at $\lambda_0 = 1550$ nm. As demonstrated at the end of Section 3, a single-polarization waveguide can also be realized with 100-nm-thick cores if only thin upper cladding is used. Such waveguides can be integrated with silicon photonics [10] to realize photonic systems that benefit from "truly single mode" operation.

Acknowledgment

The authors would like to thank LioniX BV and Aurrion, Inc. for 40- and 100-nm-thick waveguide fabrication, respectively. The authors thank Scott Rodgers, Bill Jacobs, Sam Dimashkie, Dennis Bevan, and Doug Meyer for helpful discussions. *The views and conclusions contained in this document are those of the authors and should not be interpreted as representing official policies of the Defense Advanced Research Projects Agency or the U.S. Government.*

References

[1] E. C. Kintner, "Polarization control in optical-fiber gyroscopes," *Opt. Lett.*, vol. 6, no. 3, pp. 154–156, Mar. 1981.
[2] K. Kikuchi and S. Tsukamoto, "Evaluation of sensitivity of the digital coherent receiver," *J. Lightw. Technol.*, vol. 26, no. 13, pp. 1817–1822, Jul. 2008.
[3] L. G. de Peralta, A. A. Bernussi, H. Temkin, M. M. Borhani, and D. E. Doucette, "Silicon-dioxide waveguides with low birefringence," *J. Quantum Electron.*, vol. 39, no. 7, pp. 874–879, Jul. 2003.
[4] K. K. Lee, D. R. Lim, H.-C. Luan, A. Agarwal, J. Foresi, and L. C. Kimerling, "Effect of size and roughness on light transmission in a Si/SiO_2 waveguide: Experiments and model," *Appl. Phys. Lett.*, vol. 77, no. 11, pp. 1617–1619, Sep. 2000.
[5] J. F. Bauters, M. J. R. Heck, D. John, D. Dai, M. Tien, J. S. Barton, A. Leinse, R. G. Heideman, D. J. Blumenthal, and J. E. Bowers, "Ultra-low-loss high-aspect-ratio Si_3N_4 waveguides," *Opt. Exp.*, vol. 19, no. 4, pp. 3163–3174, Feb. 2011.
[6] R. A. Bergh, H. C. Lefevre, and H. J. Shaw, "Single-mode fiber-optic polarizer," *Opt. Lett.*, vol. 5, no. 11, pp. 479–481, Nov. 1980.
[7] J. R. Feth and C. L. Chang, "Metal-clad fiber-optic cutoff polarizer," *Opt. Lett.*, vol. 11, no. 6, pp. 386–388, Jun. 1986.
[8] A. Morand, C. Sanchez-Pèrez, P. Benech, S. Tedjini, and D. Bosc, "Integrated optical waveguide polarizer on glass with a birefringent polymer overlay," *IEEE Photon. Technol. Lett.*, vol. 10, no. 11, pp. 1599–1601, Nov. 1998.
[9] P. G. Suchoski, T. K. Findakly, and F. J. Leonberger, "Low-loss high-extinction polarizers fabricated in LiNbO3 by proton exchange," *Opt. Lett.*, vol. 13, no. 2, pp. 172–174, Feb. 1988.
[10] J. F. Bauters, M. L. Davenport, M. J. R. Heck, J. Gleason, A. Chen, A. W. Fang, and J. E. Bowers, "Integration of ultra-low-loss silica waveguides with silicon photonics," in *Proc. IEEE Photon. Conf.*, 2012, pp. 701–702.
[11] D. Dai, J. Bauters, and J. E. Bowers, "Passive technologies for future large-scale photonic integrated circuits on silicon: Polarization handling, light non-reciprocity and loss reduction," *Light—Sci. Appl.*, vol. 1, pp. 1–12, 2012.
[12] D. Dai, Z. Wang, N. Julian, and J. E. Bowers, "Compact broadband polarizer based on shallowly-etched silicon-on-insulator ridge optical waveguides," *Opt. Exp.*, vol. 18, no. 26, pp. 27 404–27 415, Dec. 2010.
[13] W. K. Burns, "Phase error bounds of fiber gyro with polarization-holding fiber," *J. Lightw. Technol.*, vol. LT-4, no. 11, pp. 8–14, Jan. 1986.
[14] J. F. Bauters, M. J. R. Heck, D. D. John, J. S. Barton, C. M. Bruinink, A. Leinse, R. G. Heideman, D. J. Blumenthal, and J. E. Bowers, "Planar waveguides with less than 0.1 dB/m propagation loss fabricated with wafer bonding," *Opt. Exp.*, vol. 19, no. 24, pp. 24 090–24 101, Nov. 2011.
[15] T. Geisler and S. Herstrm, "Measured phase and group birefringence in elliptical core fibers with unparalleled systematically varied ellipticities," presented at the Eur. Conf. Opt. Commun. (Opt. Soc. Amer.), Geneva, Switzerland, 2011, Paper Th.12.LeCervin.1.
[16] A. Ourmazd, M. P. Varnham, R. D. Birch, and D. N. Payne, "Thermal properties of highly birefringent optical fibers and preforms," *Appl. Opt.*, vol. 22, no. 15, pp. 2374–2379, Aug. 1983.
[17] M. P. Varnham, D. N. Payne, A. J. Barlow, and E. J. Tarbox, "Coiled-birefringent-fiber polarizers," *Opt. Lett.*, vol. 9, no. 7, pp. 306–308, Jul. 1984.
[18] K. Takada and S. Mitachi, "Measurement of depolarization ratio and ultimate limit of polarization crosstalk in silica-based waveguides by using a POLCR," *J. Lightw. Technol.*, vol. 16, no. 4, pp. 639–645, Apr. 1998.